Mediterranean Marine Science

Vol 23, No 1 (2022)

VOL 23, No 1 (2022)

In situ experiments on the effect of low pH on the ultrastructure of the seagrasses Cymodocea nodosa and Posidonia oceanica

MARIA KOUTALIANOU, MARIA CRISTINA BUIA, CHRISTOS KATSAROS

doi: 10.12681/mms.26314

Research Article

Mediterranean Marine Science
Indexed in WoS (Web of Science, ISI Thomson) and SCOPUS
The journal is available on line at http://www.medit-mar-sc.net
www.hcmr.gr
DOI: http://doi.org/10.12681/mms.26314

In situ experiments on the effect of low pH on the ultrastructure of the seagrasses *Cymodocea nodosa* and *Posidonia oceanica*

Maria KOUTALIANOU[1], Maria Cristina BUIA[2] and Christos KATSAROS[1]

[1] National and Kapodistrian University of Athens, Department of Biology, Athens 157 84, Greece
[2] Stazione Zoologica Anton Dohrn, Villa Comunale, 80121, Naples, Italy

Corresponding author: Christos KATSAROS; christos.katsaros@biol.uoa.gr

Contributing Editor: Sotiris ORFANIDIS

Received: 6 March 2021; Accepted: 19 October 2021; Published online: 28 January 2022

Abstract

The present study investigates the impacts of low pH on the cell structure of the seagrasses *Posidonia oceanica* (L.) Delile and *Cymodocea nodosa* (Ucria) Ascherson. The study was conducted via *in situ* experiments performed at the Castello Aragonese of Ischia (Naples, Italy), where shallow submarine vents lower the pH and can be used as natural laboratories. Shoots of the seagrasses were transferred from the control area (pH 8.1) to the two venting areas (pH 7.8 and 6.8) at different times. Epidermal cells of young leaves were examined using transmission electron microscopy (TEM) and tubulin immunofluorescence. After one week at pH 7.8, the cell structure of *Posidonia oceanica* was normal, while in *Cymodocea nodosa*, microtubule (MT) network and cell structure were affected. In addition, in *C. nodosa*, ultrastructural analysis revealed a gradual degradation of the nuclei, a disorganization of the chloroplasts, and an increase in the number of mitochondria and dictyosomes. The exposure of both plants for 3 weeks at pH 6.8 resulted in the aggregation and finally in the dilation of the endoplasmic reticulum (ER) membranes. Tubulin immunofluorescence revealed that after three weeks, the MT cytoskeleton of both plants was severely affected. All these alterations can be considered as indications of an apoptotic-like programmed cell death (AL-PCD), which may be executed in order to regulate stress response.

Keywords: Plant cell ultrastructure; Ocean Acidification; Transmission electron microscopy; Programmed cell death; Microtubules; underwater vents.

Introduction

Several studies have been recently conducted on the impact of ocean acidification (OA) on marine species (Hall-Spencer *et al*., 2008; Pergent *et al*., 2014; Porzio *et al*., 2013; Kumar *et al*., 2020). The dissolution of CO_2 causes ocean acidification, and as a result, ocean water becomes less basic. This process interferes with a range of biological processes including growth, calcification and reproduction, as well as organisms' survival and behavior (Orr *et al*., 2005; Kroeker *et al*., 2010). It is estimated that by the year 2100 the ocean's surface pH will be decreased by 0.203-0.310 units (IPCC, 2013; IPCC, 2021), a fact that could be deleterious to several marine taxa (Mora *et al*., 2013). Although the exact effects of OA are still debated, there are serious questions about its potential impact on some organisms, especially those with a calcareous skeleton (Gattuso *et al*., 2013). It is suggested that some taxa may become extinct (Carpenter *et al*., 2008; Uthicke *et al*., 2013), while others may be able to cope with OA (Ries *et al*., 2009; Fabricius *et al*., 2011; Johnson *et al*., 2012; Koch *et al*., 2013).

According to Harley *et al*. (2012), non-calcifying seaweeds and seagrasses will confront both positive and negative effects from OA. It has been hypothesized that some plant processes such as growth and photosynthesis will be enhanced (Keser *et al*., 2005; Koch *et al*., 2007; Kroeker *et al*., 2010; Reusch, 2013; Koch *et al*., 2013). On the other hand, calcareous forms like coralline macroalgae may decline or vanish completely (Reusch, 2013). A number of studies have been done on calcareous species and how they can acclimatize, grow and calcify in such conditions (Porzio *et al*., 2011; Cornwall *et al*., 2013).

Seagrass meadows constitute indispensable parts of complex marine ecosystems, providing important ecological services to them (Beal & Schmit, 2000). Their distribution is affected worldwide by global climate changes and several anthropogenic activities in the coastal zone (Orth *et al*., 2006), causing an estimated 29% decrease (Waycott *et al*., 2009). However, the macrophytic responses to ocean acidification are species-specific, even among closely related species, due to variations in car-

bon acquisition strategies from seawater (Wu *et al*., 2008; Mackey *et al*., 2015) or nutrient uptake (Harley *et al*., 2012; Scartazza *et al*., 2017).

The Mediterranean marine flora is mainly characterized by the seagrass *Posidonia oceanica* (L.) Delile, an endemic marine plant which, together with *Cymodocea nodosa* (Ucria) Ascherson, supports highly complex and diverse associated communities (Mazzella *et al*., 1989; Mascaró *et al*., 2009; Tsioli *et al*., 2021). However, the increase in extreme events such as heatwaves (Easterling *et al*., 2000) can affect the persistence of these complex systems, mainly where they occur in enclosed waters (Pergent *et al*., 2014). Therefore, the acclimation responses of these two seagrasses to the effects of global climate can be relevant for the persistence of the complex ecosystems they form (Ondiviela *et al*., 2014).

There are currently available publications reporting the effects of extreme abiotic factors (mainly salinity, light and temperature) on the distribution, morphology, growth, and photosynthesis of different seagrass species (Barber & Behrens,1985; Jagels & Barnabas, 1989; Iyer & Barnabas, 1993; Lee & Dunton, 1997; Ralph *et al*., 1998; Benjamin *et al*., 1999; Serra *et al*., 2013; York *et al*., 2013). In addition to the above, there are several papers that report the effect of OA on the structure of marine plant ecosystems (Vizzini *et al*., 2010; Jiang *et al*., 2010; Porzio *et al*., 2011; Arnold *et al*., 2012; Apostolaki *et al*., 2014, Garrard *et al*., 2014).

However, there is currently no information on the effects of OA on the cell fine structure and cytoskeleton organization of seagrasses, although there are publications on the effect of biotic and abiotic stress on the cytoskeleton and fine structure of *C. nodosa* (Malea *et al*., 2013; Koutalianou *et al*., 2016; Adamakis *et al*., 2018; Mylona *et al*., 2020a; Mylona *et al*., 2020b; Adamakis *et al*., 2021). The only data on the effect of OA on cell fine structure are reported in studies dealing with coral species, i.e., *Pocillopora damicomis* and *Oculina patagonica* (Kvitt *et al*., 2015). In the first species, after incubation at pH 7.2 for 2-4 weeks, necrotic cells characterized by ruptured cell membranes appeared, while in the latter species, apoptotic cells characterized by nuclear chromatin forming crescent-like caps were observed (Kvitt *et al*., 2015). The biochemical pathways are not well studied, so it is difficult to integrate the fields of seagrass ecophysiology and ecogenomics (Procaccini *et al*., 2012). Therefore, there is an urgent need to develop tools to assess and quantify OA impacts across the entire range of biological responses, from the subcellular level to ecosystem reorganization, and from short-term physiological acclimation to evolutionary adaptation (Riebesell, 2008).

The aim of the present study was to investigate the impacts of pH lowered from current levels on the cell structure in both *Posidonia oceanica* and *Cymodocea nodosa*. The study was conducted via *in situ* experiments at the Castello Aragonese of Ischia Island (Italy), where naturally CO_2-venting sites alter the chemical composition of the surrounding water. Our report is, to the best of our knowledge, the first study focused on the possible effects of acidification on seagrass cell ultrastructure.

Materials and Methods

Study Sites

The study was carried out on the south side of the Castello Aragonese on the island of Ischia (Italy, 40.731447° N, 13.966089° E), where underwater vents occur within an area of about 3000 m^2 (Hall-Spencer *et al*., 2008). The gas emissions are mainly composed of CO_2, with undetectable concentrations of trace elements and no hydrogen sulfide (Tedesco, 1996; Hall-Spencer *et al*., 2008; Kroeker *et al*. 2011). These CO_2 vents produce a pH gradient that can be used to study the natural effects of acidified seawater on benthic organisms, since there are no confounding gradients of temperature, salinity, hydrodynamic conditions, and toxic hydrogen sulfide (Ravaglioli *et al*., 2017; Hall-Spencer *et al*., 2008; Kerrison *et al*., 2011; Foo *et al*., 2018). The pH gradient ranges from current ambient level (ca. 8.1.) in S1 to 7.8 (the near future change in ocean pH) in S2 to 6.8 in the area with more intense venting (S3). The pH values in the study area can vary daily in accordance with the intensity of vent activity and water movements but are quite stable over the long term (Porzio *et al*., 2011) (Suppl. Fig. 1).

Collection of Posidonia oceanica and *Cymodocea nodosa*

The study was conducted in June and July of 2014. In June, *P. oceanica* and *C. nodosa* shoots were collected by SCUBA diving at current pH (S1) in a close area at approximately 2 m depth where both seagrasses grow. In this area, twelve shoots of each species were collected randomly; three shoots of each species were fastened to a plastic net and fixed with iron bars at areas with lower pH (both S2 and S3) (Suppl. Fig. 2). In order to test the transplantation effect, both seagrasses were also transplanted within the same collection site. After 1 and 3 weeks, transplanted shoots were removed, and the smallest juvenile leaves (less than 5 cm long) were carried to the lab. Also, shoots of *P. oceanica* naturally occurring within the S2 (pH 7.8) area were collected for comparison with the shoots had been transplanted from S1 (8.1) to S2 (7.8).

The leaf parts used in all the experiments were taken from either the smallest juvenile leaf or the second smallest juvenile leaf of both *P. oceanica* and *C. nodosa.* This leaf category was chosen (according to a previous study by Koutalianou *et al*., 2016) because it displays many mitotic cells. Specifically, small pieces of juvenile leaves (0.5 cm height × 0.3-0.7 cm length) were cut and used for the experiment. Similar to previous experiments with *C. nodosa* (Koutalianou *et al*., 2016), the present study was focused on the epidermal cells, which are the main photosynthetic sites of the seagrasses (Kuo & den Hartog, 2006). To distinguish transplantation from pH effects, control shoots were examined in parallel.

Environmental data

As the vent activity does not heat the water (Kerrison *et al*., 2011), there were no thermic differences among the three sites. The temperature was continuously monitored using a HOBO data logger, which was positioned on the bottom (2 m depth) to record the temperature regime during the experiment. In addition, pH measurements were taken for the duration of the experiment; water collected from each site weekly (in June and July) was carried in dark conditions to the lab. pH measurements were taken using a Mettler Toledo SG2 pH meter (USA), which measures 0.01 units, is equipped with an InLab 413 electrode, and is calibrated regularly using NIST-traceable buffers. Although this approach does not measure the total hydrogen ion concentration, it does measure the relative change in pH between sites (precision within 0.01 pH units).

Electron microscopy

For the preparation of the material for transmission electron microscopy (TEM) study, the protocol reported by Katsaros *et al*. (1983) was followed. Thin sections of epidermal cells were examined with a Philips 300 and a JEOL 100S TEM (Japan).

Indicatively, the number and size of the mitochondria and chloroplasts were measured on micrographs taken from serial sectioning of the cells. The average number and size of the mitochondria and chloroplasts were plotted as histograms using MS Excel software (Microsoft Corp.). Standard deviation (SD) bars were used. At least 100 interphase young epidermal cells from 3 different shoots from each experiment area were used for the measurements.

Tubulin immunofluorescence

Tubulin immunofluorescence was applied on meristematic cells following a modified protocol of Katsaros & Galatis (1992). A modified enzyme solution for the softening of the cell walls was used. The solution contained 2.5% (w/v) cellulase Onozuka (Yakult Honsha Co., Tokyo, Japan), 2% (w/v) macerozyme Onozuka (Yakult), 1% (w/v) driselase from *Basidiomycetes* sp. (Sigma, St. Louis, MO, USA), and 1% (v/v) β-glucuronidase type HP-2 from *Helix pomatia* (Sigma) in PEM buffer (0.1 mM Pipes, 2 mM EGTA, 1 mM magnesium sulfate) in a solution with pH of 5.6. Cell wall softening was conducted for 80 min. Following rinsing with PEM, the leaves were squashed on coverslips coated with 1 mg/mL poly-L-lysine (Sigma) and left to allow the separated cells to dry. For the tubulin labeling, both anti-a-tubulin (YOL1/34, AbD Serotec, Kidlington, UK) and FITC-anti-rat secondary antibody (Sigma) diluted at a concentration of 1:40 were used. DNA was counterstained with 10 μg/mL Hoechst 33258 (Sigma), and the cells or small leaf pieces were finally mounted in an anti-fade solution of 1.6 mg/ml p-phenylenediamine (Sigma) diluted in a solution containing 2:1 glycerol:PBS. The samples were examined with a Zeiss 510 Meta confocal microscope.

Results

Environmental data

During the transplantation experiments, the water temperature ranged between 22.8 ± 1.5 and 24.7 ± 0.9 °C, in June and July, respectively, matching ambient seasonal fluctuations (13-25°C) (Suppl. Fig. 3). During the transplantation experiments, the pH values at S1, S2 and S3 were 8.08 ± 0.004, 7.71 ± 0.133 and 6.584 ± 0.145, respectively (Suppl. Fig. 4).

Fine structure of young epidermal cells of control material (pH 8.1- S1)

In paradermal sections of young leaves of *C. nodosa*, epidermal cells usually appeared rectangular or orthogonal in shape. Due to repeated cross divisions, their axis parallel to the leaf axis was shorter than the other one (average dimensions 40x70 μm, SD 0.5). They were characterized by a large nucleus occupying most of the cell space (Fig. 1A). The few dense masses of condensed chromatin were usually distributed along the nuclear periphery, while a prominent nucleolus was present in a central position (Fig. 1A). The cytoplasm was dense, with a few vacuoles. Chloroplasts were oval-shaped in sections, with a limited number of thylakoids and developing grana. Mitochondria, endoplasmic reticulum (ER) and dictyosomes were also occasionally present (Fig. 1A, B).

Similar sections of *P. oceanica* leaves revealed that young epidermal cells were mainly orthogonal, with average dimensions of 45x90 μm (SD 0.6). The nucleus was round, with an abundant network of condensed chromatin (Fig. 2 A, B). Well-sized vacuoles occupied a significant part of the cell space. Undifferentiated, variably-shaped chloroplasts with large plastoglobuli were distributed in the cell cortex. ER and mitochondria were usually peripherally arranged (Fig. 2C). For comparison purposes, paradermal sections of young leaves of *P. oceanica* that naturally occurred within area S2 were examined and revealed a cell structure similar to that described above.

Tubulin immunofluorescence of control material revealed that the MT cytoskeleton of interphase epidermal cells in both seagrasses was organized in parallel bundles oriented more or less perpendicularly to the long leaf axis.

Effect of acidification on the cell structure

One week in S2 area (pH 7.8) and in S3 area (pH 6.8)

One week after transfer from the control area (S1, pH 8.1) to the S2 area (pH 7.8), *C. nodosa* shoots appeared

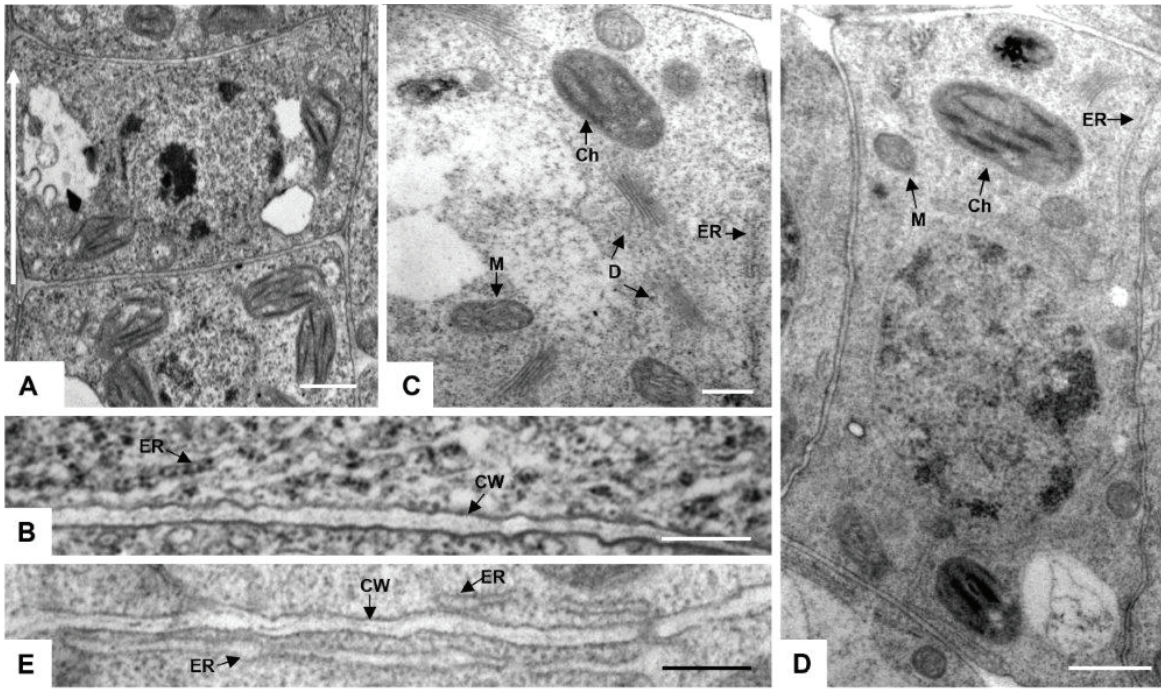

Fig. 1: **A-E.** TEM micrographs of young epidermal cells of *C. nodosa* control material**. A.** Paradermal section of an epidermal cell. Note its orthogonal shape, the dense cytoplasm, and the large nucleus occupying most of the cell space. **B**. Higher magnification of the peripheral part of the cell of Fig. A, showing the cell wall and cortical endoplasmic reticulum (ER). **C.** Cytoplasmic area taken from a plant transferred for one week to S1 area. Note the increased number of mitochondria, dictyosomes and ER, compared to the control. **D.** Epidermal cell after transfer for one week from S1. It shows a prominent central nucleus, undifferentiated chloroplasts with few grana and an increased number of mitochondria and ER membranes. **E.** Higher magnification of a cortical cytoplasmic area of a cell like D showing an extended ER network distributed in the cell periphery. *Scale bars = 2 μm (A), 1μm (D) and 0.2μm (B, C, E).*

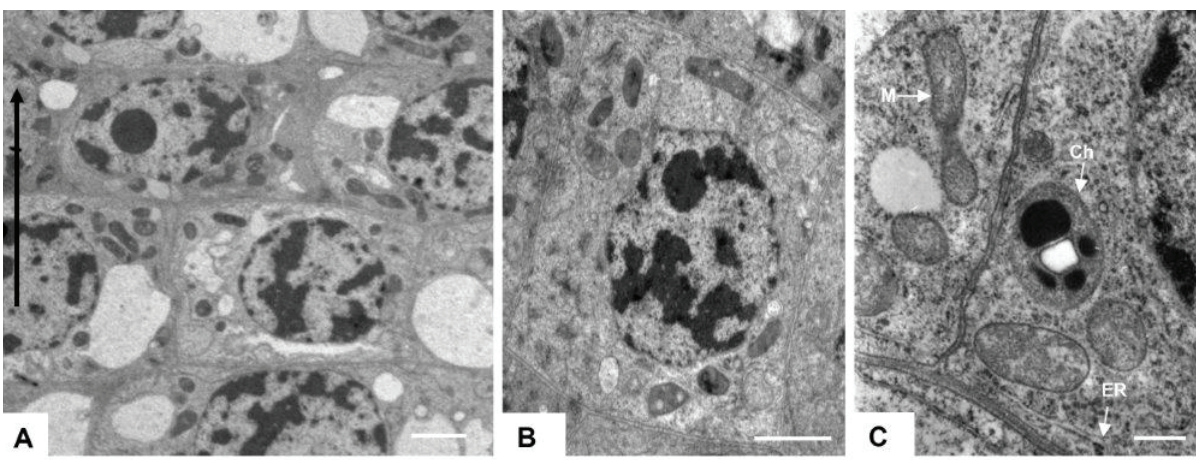

Fig. 2: **A-C.** TEM micrographs of young epidermal cells of *P. oceanica* control material**. A.** Epidermal cells orthogonal in shape, with dense cytoplasm and a round-shaped nucleus. The arrow marks the direction towards the leaf apex. **B**. Higher magnification of a nucleus with an impressive network of condensed chromatin. **C.** Undifferentiated chloroplast with large plastoglobuli. ER and mitochondria are also positioned in the cell periphery. *Scale bars = 2 μm (A), 1μm (B) and 0.5μm (C).*

healthy, with no obvious effects on their external structure. Immunofluorescence preparations of young epidermal cells showed a disturbance of interphase MTs, which appeared short and fragmented, with a loss of proper orientation (Fig. 3A). Examination of young epidermal cells under TEM revealed that their structure was not severely affected. However, a few alterations in comparison to the control were observed:

a. The number of mitochondria increased considerably (Fig. 1C, D, Suppl. Fig. 5); however, their elliptical shape and their structure were normal, with well-organized cristae (Fig. 1C).
b. ER was also increased, with extended cisternae mainly distributed in the cell periphery (Fig. 1D, E).
c. The number of dictyosomes also appeared to have increased (Suppl. Fig. 6), showing an increased number of cisternae (Fig. 1C, Suppl. Fig. 7).
d. Chloroplasts appeared undifferentiated, with a few grana (Fig. 1C, D).

Transplantation of *C. nodosa* from the S1 area (pH

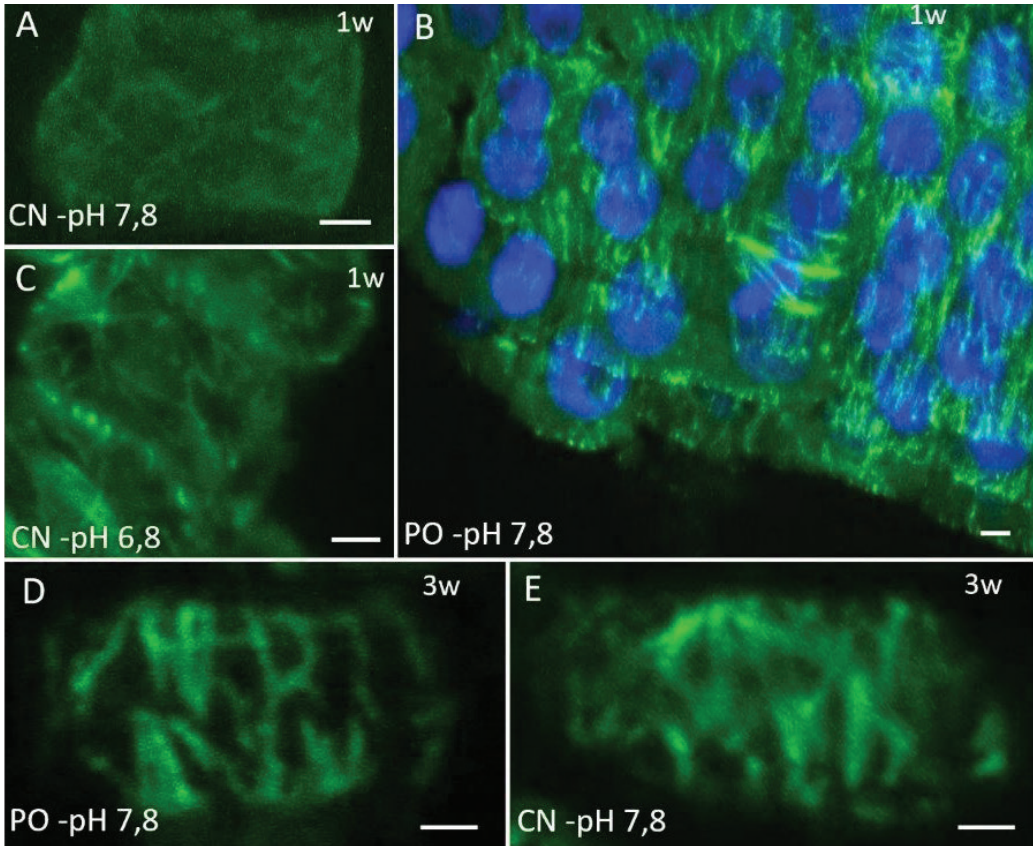

Fig. 3: **A-E.** Interphase epidermal cells of young leaves under different pH levels. In all figures, green represents tubulin immunofluorescence and blue represents Hoechst staining of DNA. **A.** Transfer of CN to pH 7.8 for 1 week: thick MT bundles showing a slightly aberrant orientation. **B**. Transfer of PO to pH 7.8 for 1 week: MT bundles oriented perpendicularly to the long leaf axis. **C.** Transfer of CN to pH 6.8 for 1 week: fragmented MT bundles with slightly aberrant orientations. **D.** Transfer of CN to pH 7.8 for 3 weeks: short, fragmented, and curved MT bundles with aberrant orientations. **E.** Transfer of PO at pH 7.8 for 3 weeks: depolymerization and disassembly of interphase MTs with loss of proper orientation. *Scale bar = 10 μm.*

8.1) to the S3 area (pH 6.8) for one week revealed similar effects in young epidermal cells as those observed at pH 7.8, but to a higher degree:

a. Mitochondria were three times more in number than the control (Suppl. Fig. 5), with very few cristae (Figs 4A, C).
b. Endoplasmic reticulum was increased, with extended and sometimes fragmented cisternae.
c. Dictyosome number, as well as the number of cisternae in each dictyosome, were also increased (Suppl. Fig. 6, Suppl. Fig. 7).
d. Chloroplasts still appeared undifferentiated, with a few grana (Figs 4A, B). Immunofluorescence examination also revealed a disturbance of interphase MTs similar to that observed above at pH 7.8 conditions. MT bundles were fragmented with loss of transverse orientation (Fig. 3C).

In *P. oceanica*, one week transplantation from the control area (S1, pH 8.1) to the S2 area (pH 7.8) had no observable effects. The structure of the cells was similar to that observed in shoots at S1. Anti-tubulin immunofluorescence examination showed that the MTs in interphase epidermal cells appeared oriented perpendicularly to the long leaf axis (Fig 3B). In contrast, after one week in the S3 area (pH 6.8), young epidermal cells of *P. oceanica* appeared to be drastically affected in the following manner:

a. Number of mitochondria was nearly doubled compared to control cells, with very few broken or swollen cristae (Figs 5A, B).
b. Chloroplasts were not increased in number, but did show increased starch content. In random sections of material from the control area, 85% of the chloroplasts showed no starch grains, while in the S3 area the percentage was less than 50%. The shape and the size of plastoglobuli were also changed compared to the control. Oval-shaped (Fig. 5A, B) and rod-like plastoglobuli were observed around starch grains (Fig. 5D).
c. Endoplasmic reticulum was extended and sometimes fragmented along the cell periphery (Fig. 5D). Interestingly, the dictyosome number and size were not influenced by this pH change (Fig. 5D). In immunofluorescence examination, the results were similar to those observed in *C. nodosa* at the same pH.

Three weeks in S2 area (pH 7.8)

Transplantation of *C. nodosa* from the control area to S2 for three weeks caused severe changes in the cell structure. The cells appeared empty, with most of the cell

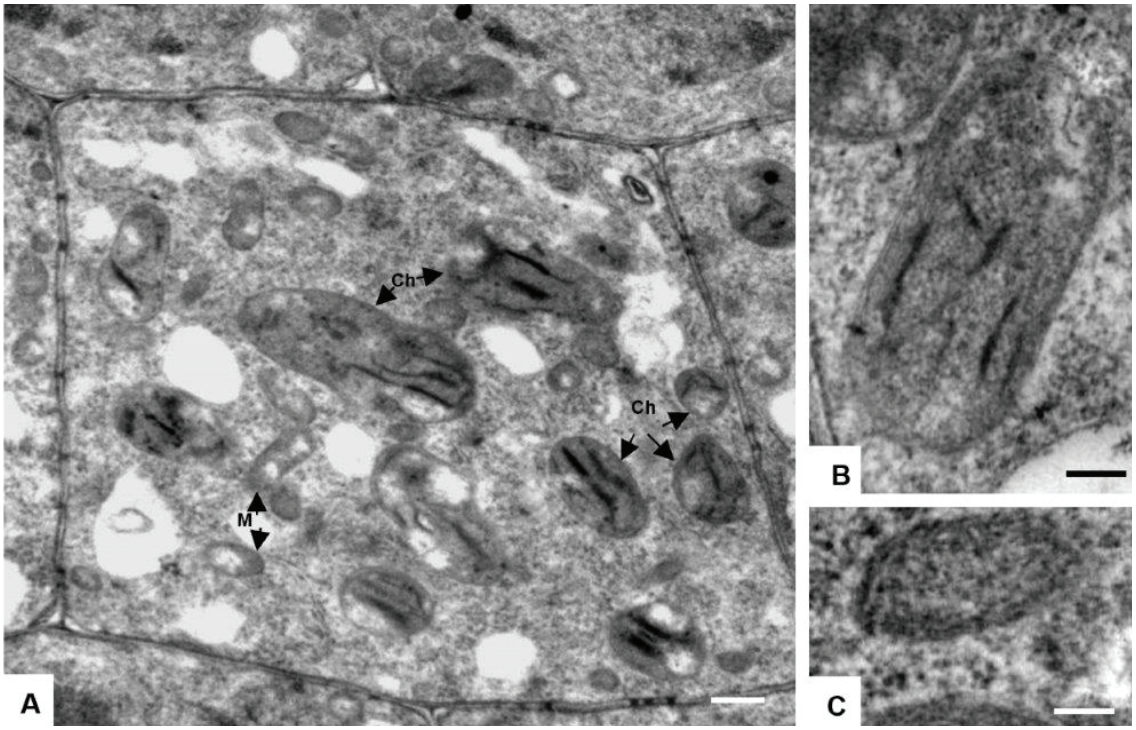

Fig. 4: **A-C.** TEM micrographs of young epidermal cells of *C. nodosa* after one week transfer at S2 area. **A**. Epidermal cell with undifferentiated chloroplasts and increased number of mitochondria. **B**. Higher magnification of a chloroplast with a few developing grana. **C**. Higher magnification of a mitochondrion with very few cristae. *Scale bars = 0.5 μm (A, B, C).*

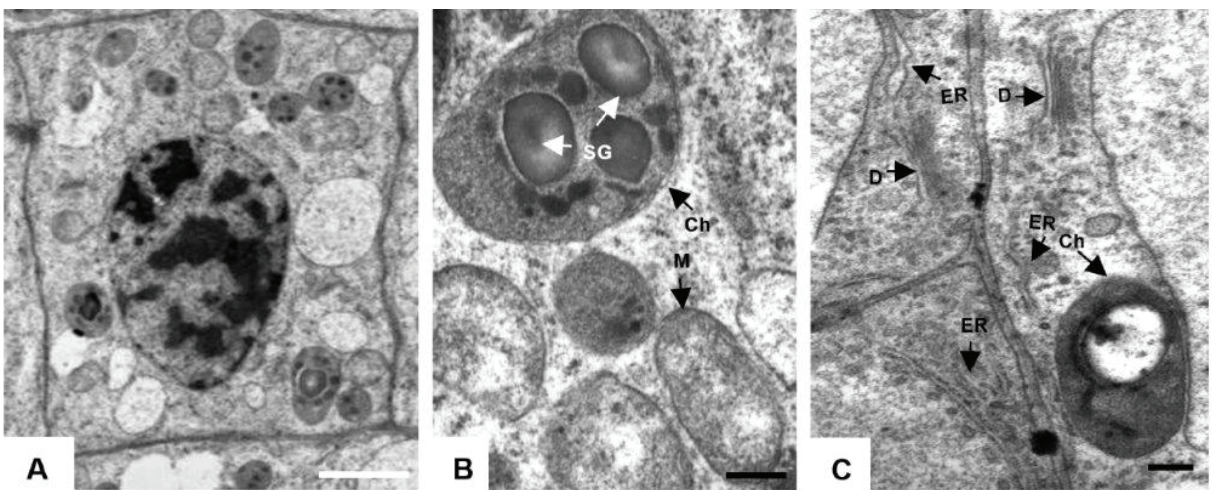

Fig. 5: **A-C.** TEM micrographs of young epidermal cells of *P. oceanica* after one week transfer at S2 area. **A**. Epidermal cell with increased number of chloroplasts and mitochondria. **B.** Chloroplast with oval-shaped and rod-like plastoglobuli around starch grains. Mitochondria with very few fragmented cristae are also visible. **C.** Dictyosomes and fragmented ER network extended along the cell periphery. *Scale bars = 1 μm (A), and 0.5μm (B, C).*

elements disorganized and distorted. Nuclei showed condensed masses of chromatin that covered most of the nucleoplasm (Figs. 6A, B). The nuclear membrane appeared loose and discontinuous (Fig. 6B). Chloroplasts were also disturbed. Their shape was rounded, and the typical thylakoid and grana organization was lost. Chloroplasts were characterized by the presence of large starch grains surrounded by a system of electron-dense elongated or round plastoglobuli (Fig. 6E). Mitochondria were numerous, with a few broken and sometimes dilated cristae (Fig. 6E). Dictyosomes with a few cisternae were distributed in the cytoplasm (Fig. 6D). In cytokinetic cells, the forming cell plate consisted of dilated and electron-dense vesicles. Endoplasmic reticulum was also affected by the low pH treatment. Numerous swollen fragments of rough ER (RER), as well as masses of electron-dense material attached to ER cisternae, were observed along the cell cortex, while fragmented ER membranes were also found in the cytoplasm (Figs 6C, D). During immunofluorescence examination, MTs of interphase cells were observed forming short, fragmented, curving bundles with loss of proper orientation (Fig 3D).

Young epidermal cells of *P. oceanica* also showed distorted cytoplasm after three weeks at pH 7.8 (S2 area). Condensed chromatin masses within nuclei were observed (Fig. 7A). Dark-stained cisternae and globules

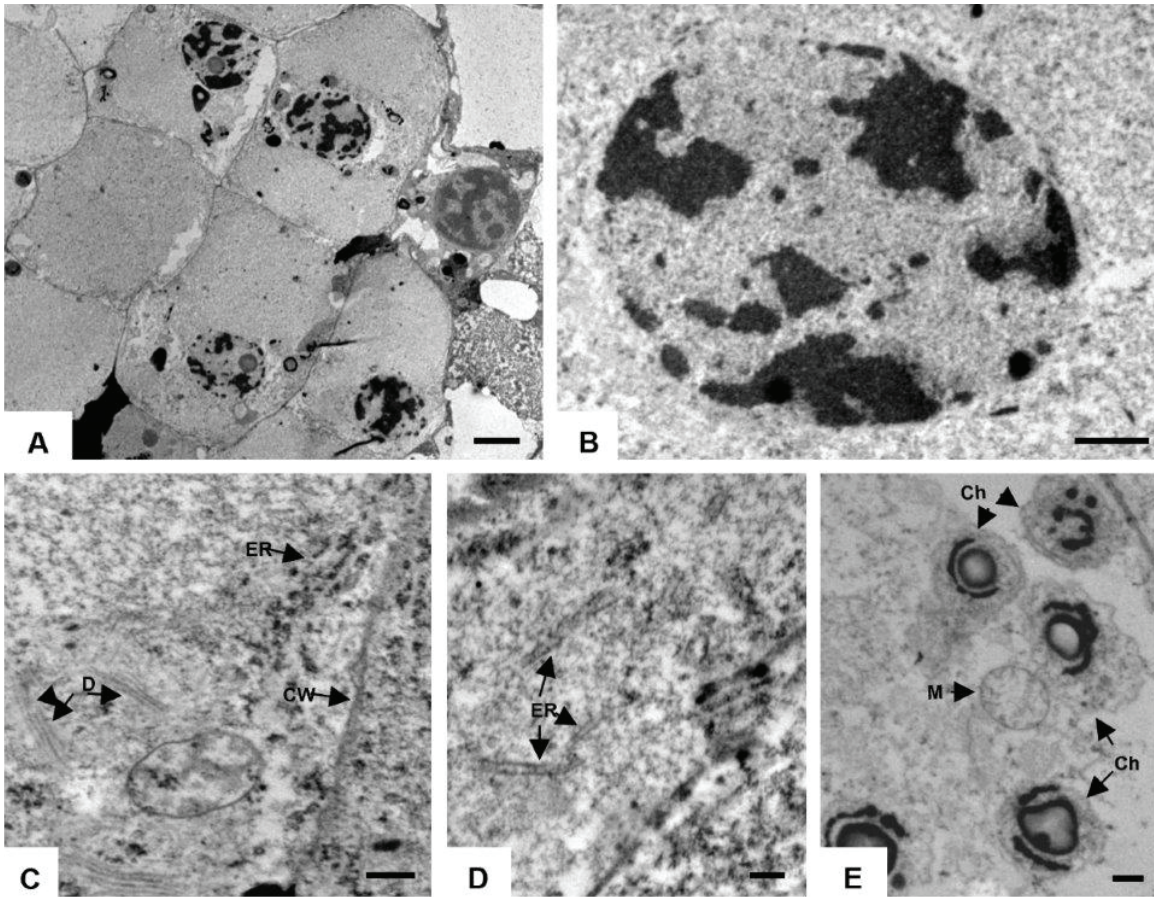

Fig. 6: **A-E.** TEM micrographs of young epidermal cells of *C. nodosa* after three weeks transfer at S1 area. **A**. Group of epidermal cells that appear empty, with most of the cell elements disorganized and distorted. **B.** Higher magnification of a nucleus with condensed masses of chromatin which covered most of the nucleoplasm. The nuclear membrane appears loose and discontinuous. **C.** Cytoplasmic area showing dictyosomes with few cisternae and numerous swollen fragments of rough ER (RER) **D.** Fragmented ER membranes traversing the cortical cytoplasm. **E.** Disorganized chloroplasts with large starch grains surrounded by a system of electron-dense elongated or round plastoglobuli. Mitochondria with a few broken and sometimes dilated cristae are also observed. *Scale bars = 1 μm (A), 0.5μm (B, C, E) and 0.2μm (D).*

within chloroplasts were also noticed (Figs 7B, C). The starch grains within the chloroplasts and the plastoglobuli appeared similar to that described above (i.e., one week at S3 area). Mitochondria seemed disorganized and empty, and the ER appeared fragmented and arranged mainly along the cell periphery (Fig. 7D). MTs of interphase cells were observed to be similar to those in *C. nodosa*, forming short, fragmented, curving bundles with loss of their orientation (Fig. 3E).

Three weeks in S3 area (pH 6.8)

Transfer of *C. nodosa* plants from the control area to S3 for three weeks also caused severe changes in the cell structure. Cells were distorted and most of the organelles not easily seen. The newly formed cell walls appeared wavy and occasionally fragmented (Fig. 8A, B). Vacuoles contained electron-dense material. Mitochondria were numerous, containing a rather amorphous mass of destroyed cristae (Figs 8C, D). Chloroplasts were empty, with remnants of thylakoids and starch grains inside them (Fig. 8E, F). The ER network was more severely affected than previously mentioned organelles with inflating, swelling and fragmented RER membranes (Figs 8F, G, H). Numerous swollen fragments of RER (Fig. 8F), as well as masses of electron-dense material attached to and forming a network with ER, were observed (Figs. 8G, H). This network appeared to have structures surrounded by a membrane similar to ER, with projected edges filled with electron-dense material. Dictyosomes were also disorganized, with swollen cisternae enclosing an amorphous mass of cytoplasmic material (Fig. 8D). MT bundles in interphase cells were organized as in the S2 area, i.e., they were severely affected.

After three weeks at pH 6.8, young epidermal cells of *P. oceanica* also appeared drastically affected, as follows:

a. Newly-formed cells had wavy cell walls (Figs. 9A, B).
b. Mitochondria were hardly distinguishable from chloroplasts, since both typically appeared empty (Fig. 9C).
c. Chloroplasts were completely destroyed, and sometimes contained remnants of thylakoids and/or ovoid plastoglobuli (Figs. 9C, D). Starch grains were dispersed in the cytoplasm (Fig. 9D).
d. The endoplasmic reticulum network displayed inflated, swollen RER cisternae, filled with elec-

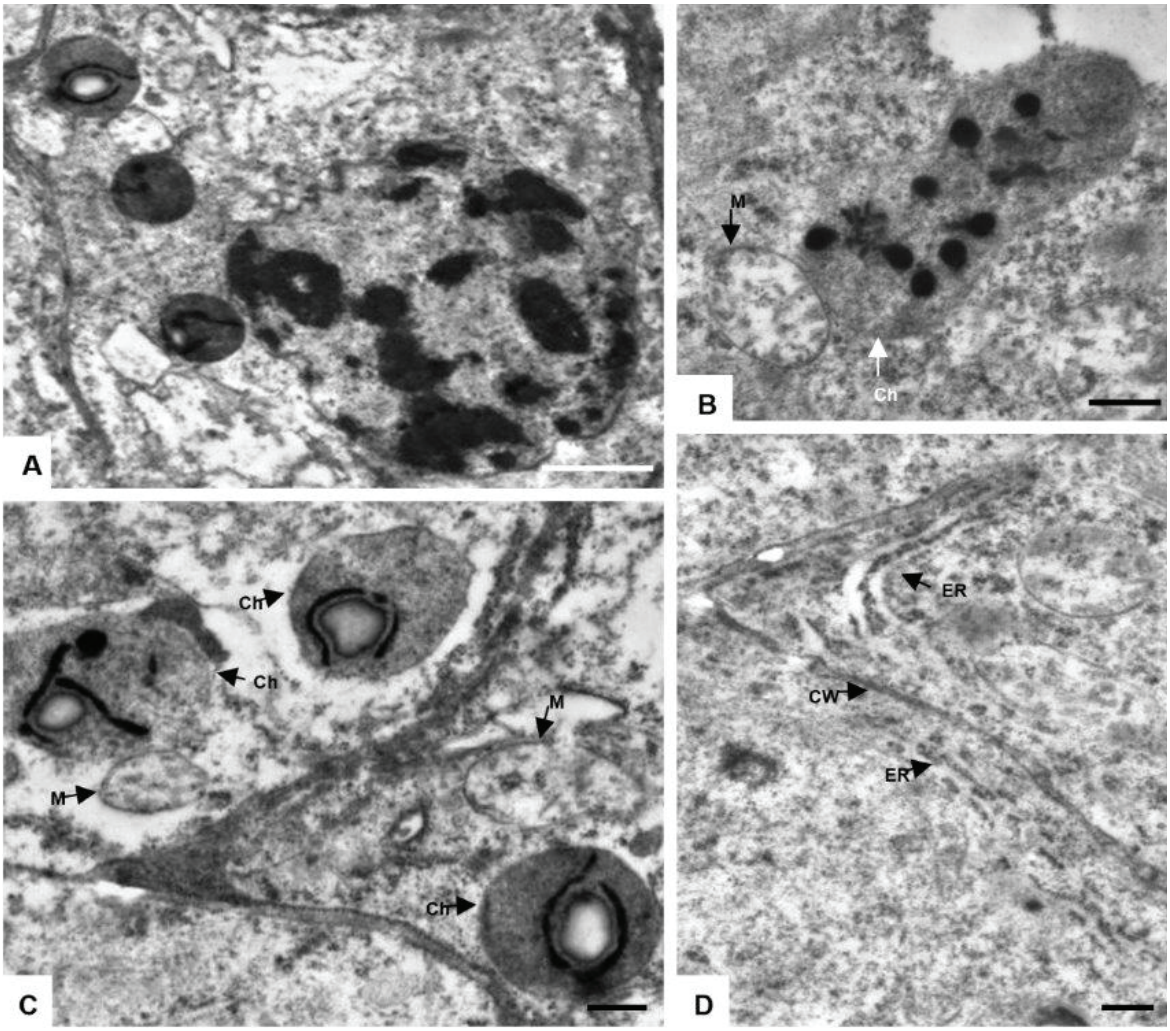

Fig. 7: **A-D.** TEM micrographs of young epidermal cells of *P. oceanica* after three weeks transfer at S1 area. **A.** Part of an epidermal cell of *P. oceanica* with warped cell walls, distorted cytoplasm, and a large nucleus with condensed chromatin masses. **B.** Chloroplast with remnants of disorganized cisternae and round plastoglobuli. **C.** Chloroplasts with large starch grains surrounded by a system of electron-dense elongated and/or round plastoglobuli. Mitochondria with a few broken dilated cristae are visible. **D.** Fragmented ER membranes arranged along the cell periphery. *Scale bars = 1 μm (A), 0.5μm (B, C) and 0.2μm (D).*

tron-dense material (Fig. 9E, F).

e. Dictyosomes were normal in shape but few in number (Fig. 9C). MT organization was severely affected, as in S2 area.

Discussion

Our results show that there is a difference between the two seagrasses in the time-lag between exposure to a lower pH and appearance of changes at the ultrastructural level. In particular, *C. nodosa* seemed to be affected more quickly (changes apparent after 1 week) than *P. oceanica* (changes apparent after three weeks). This pattern seems to be in accordance with the different ecological roles of the two species. The climax species *P. oceanica* seems to be more resilient to environmental changes such as those related to the increase in CO_2, compared to the pioneer species *C. nodosa*, for which a more immediate response to changes such as those related to temperature and light has been demonstrated (Cancemi *et al*., 2002). However, differences between the two seagrasses may also be due to their different seasonal growth rates. *Cymodocea nodosa* has high growth rates in summer (the period of our experiment) (Cancemi *et al*., 2002), and consequently it should be more metabolically active; in contrast, *P. oceanica* is less active during the same period, with the lowest monthly rate of new leaf appearance in summer (Buia *et al*., 1992; Zupo *et al*., 1997).

Of particular interest among our results is the relevance of duration of exposure to low pH in causing damage. This was demonstrated by differences between *P. oceanica* that had been acclimated to the S2 area (Hall-Spencer *et al*., 2008; Garrard *et al*., 2014; Foo *et al*., 2018) and *P. oceanica* that had been transferred from S1 to S2 for 3 weeks. The cell structure of the transplanted shoots in the S2 area was affected while the acclimated plants were not. This reveals that *P. oceanica* is influenced differently based on the time available for acclimation; *P. oceanica* plants that were currently living at normal pH (8.1, S1) and exposed for some weeks to low pH (7.8, S2) were more damaged than plants living for decades at lower pH (Hall-Spencer *et al*., 2008).

The fine structure of young epidermal cells of

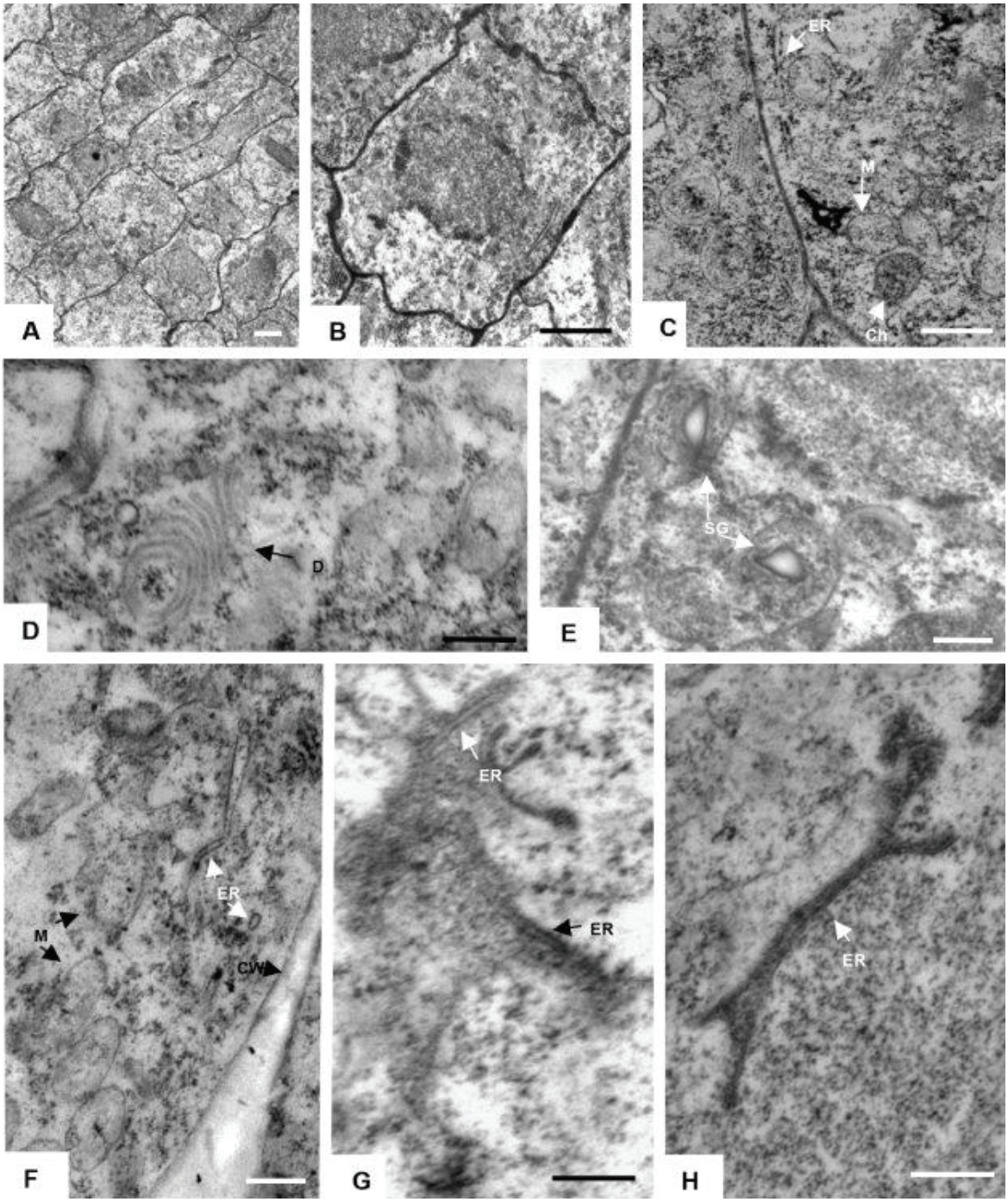

Fig. 8: **A-H.** TEM micrographs of young epidermal cells of *C. nodosa* after three weeks transfer at S2 area. **A.** Surface view of epidermal cells. They are disorganized and most of the organelles are not easily seen. **B.** Epidermal cell with wavy cell walls and a central nucleus with loose and partially disrupted nuclear membrane. **C.** A group of peripherally distributed mitochondria containing a rather amorphous mass of destroyed cristae. **D.** Dictyosome with rounded and loose cisternae. **E.** Disorganized chloroplasts with remnants of thylakoids and starch grains. **F.** Cortical cytoplasmic area with disorganized mitochondria and inflated ER fragments. **G.** Higher magnification of inflated fragments of RER with attached electron-dense material. **H.** ER membrane-like network with projecting edges filled with electron-dense material. *Scale bars = 2 μm (A), 1μm (B) 0.5μm (C), 0.2 (D, E, F) and 0.1 (G, H).*

P. oceanica leaves currently growing in pH 7.8 was similar to that occurring in plants growing at pH 8, as well as that reported by several authors such as Doohan & Newcomb (1976), Barnabas (1977), Kuo (1978, 1990, 1993) and Kuo & den Hartog (2006). The main structural characteristics of these cells (i.e., the large nucleus with condensed chromatin and the undifferentiated chloroplasts, which often appear to be dividing) are consistent with their meristematic character (Papini *et al*., 1999). The repeated divisions do not allow for the differentiation of the cells. The MT organization in interphase cells of *C. nodosa* and *P. oceanica* at pH 7.8 was similar to that reported by other studies of seagrasses (Malea *et al*., 2013; Koutalianou *et al*., 2016).

The exposure of *C. nodosa* and *P. oceanica* plants to a pH lower than normal (7.8 and 6.8) for three weeks

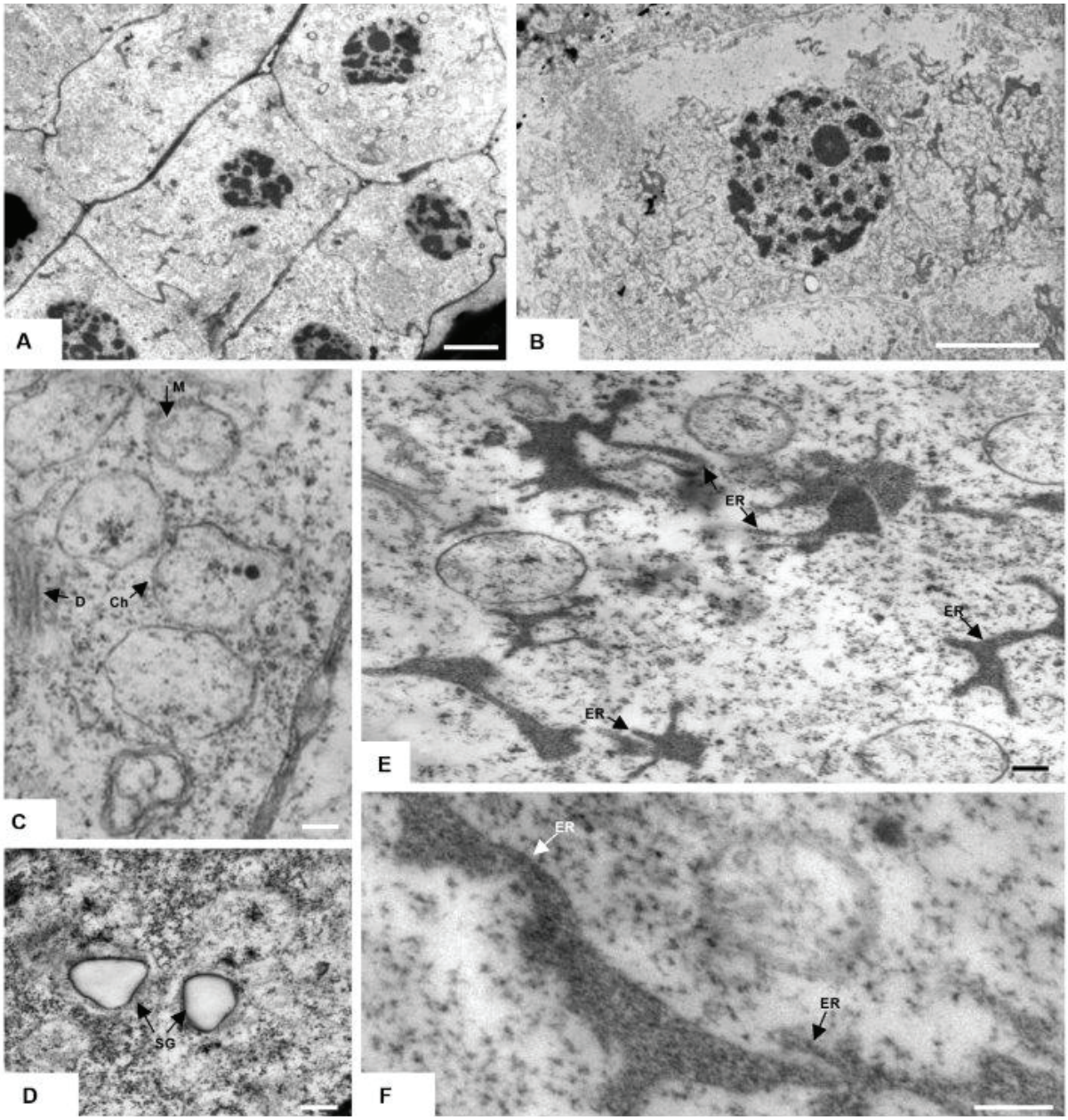

Fig. 9: **A-F.** TEM micrographs of young epidermal cells of *P. oceanica* after three weeks transfer at S2 area. **A.** Group of epidermal cells that appear distorted, with wavy cell walls. **B.** Part of an epidermal cell with a central nucleus with disorganized nuclear membrane. The nucleus is surrounded by remnants of cell organelles and an electron-dense ER network. **C.** Chloroplasts with remnants of thylakoids and plastoglobuli, and disorganized mitochondria. Both appear empty and destroyed. **D.** Starch grains from disorganized chloroplasts appear dispersed in the cytoplasm. **E.** Cytoplasmic area with structures of ER network connected and/or filled with electron-dense material. **F.** Higher magnification of inflated, swollen RER cisternae, filled with electron-dense material. *Scale bars = 2 μm (A), 1μm (B) 0.2 (C, D, E,) and 0.1 (F).*

caused a gradual degradation of the nuclei, which was indicated by the formation of masses of condensed chromatin. This could be considered as a symptom of programmed cell death (PCD) as previously reported in plants, where PCD-activated nucleases cleave DNA at linker sites between nucleosomes, resulting in DNA fragmentation (Reape *et al*., 2008).

The predicted positive effect of ocean acidification on some physiological processes of seagrasses, such as growth rate and photosynthetic efficiency (Beer & Koch, 1996; Larkum *et al*., 2006), does not always find the same consensus like variable effects of ocean acidification demonstrated on different marine organisms (Kroeker *et al*., 2011). Studies conducted in sites characterized by underwater vents can give give different results based on species, site, or geochemical conditions. *Posidonia oceanica* plants growing normally in CO_2-enriched conditions at ambient temperature have demonstrated that the maximum photochemical efficiency of photosystem II is unaffected by a loss of the CO_2 limitation (Hall-Spencer *et al*., 2008; Scartazza *et al*., 2017; Hendriks *et al*., 2017; Vizzini *et al*., 2010), while the growth depends upon nutrient concentration (Ravaglioli *et al*., 2017). An opposite trend has been recorded for populations of *C. nodosa* naturally exposed over the long-term to acidified water, for which photosynthetic activity seems to be promoted by

low pH (Apostolaki *et al*., 2014).

The length of exposure is probably responsible for differences in acclimation. In our study, short term transfers are responsible for the disorganization of the chloroplasts, testified by the loss of their internal membrane organization. Similar responses under stress conditions have been reported for terrestrial plants, such as in cotton cells under cadmium treatment (Daud *et al*., 2009), cucumber and soybean cold-treated cells (Lee *et al*., 2002; Glinska *et al*., 2009), and *N. tabacum* callus cells under salt stress (Bennici *et al*., 2012). The disorganization of chloroplasts in meristematic cells (especially after 3 weeks at pH 6.8) found in the present study could be explained by the translocation of photosynthates from aboveground to belowground tissues, which has been shown to decrease the leaf chlorophyll content of *Thalassia hemprichii* under elevated CO_2 conditions (Jiang *et al*., 2010). The appearance of osmiophilic (globular or rod-like) structures after prolonged treatment with low pH observed in our seagrasses is quite common in cells undergoing biotic and abiotic stress. It has been suggested that plastoglobuli participate in the plant stress response (Eymery & Rey, 1999; Kanwischer *et al*., 2005; Austin *et al*., 2006; Grigorova *et al*., 2012).

In addition to chloroplast membrane degradation, exposure to low pH for three weeks resulted in starch depletion in *P. oceanica* and *C. nodosa*. This low starch content in leaves has been already detected in the *P. oceanica* population naturally growing at 7.8 pH, where it was also associated with a low C:N ratio; in contrast, the starch content of the rhizomes was not affected by low pH (Scartazza *et al*., 2017). The starch depletion observed in the leaves in this study is in accordance with previous studies using different stress treatments (Grigorova *et al*., 2012) and supports the hypothesis that starch degradation products could be agents involved in stress tolerance (Le Rudulier *et al*., 1984).

Another important finding of the present study is the increase in the number of mitochondria, accomplished by cristae disorganization. Similar observations have been reported for root cells of two soybean cultivars after cold treatment (Glinska *et al*., 2009) and in lupine embryo cells under salinity stress (Wojtyla *et al*., 2013). In Al-treated tobacco cells, mitochondria swelling has been attributed to osmotic changes in the local environment (Mannela, 2008) and an increase in Reactive Oxygen Species (ROS) levels, which lead to an increase in mitochondrial membrane permeability (Li & Xing, 2011). This is due to opening of the mitochondrial permeability transition pore (MPT) induced by calcium, which may cause a PCD event (Panda *et al*., 2008). Mitochondria, together with chloroplasts, are involved in the regulation of cellular homeostasis and have been considered major (ROS) producers (Rurek *et al*., 2014). It has also been reported that alterations in the internal structure of mitochondria could be attributed to a higher level of ADP (relative to ATP) due to inhibition of oxidative phosphorylation. This agrees with the results of Kvitt *et al*. (2015) and Wei *et al*. (2015), who studied the effect of high pCO_2 in oyster tissues. They suggested that oyster gills may overcome the stress induced by elevated pCO_2 by consuming more ATP.

The endoplasmic reticulum has been proved to be sensitive to a variety of stresses, including chilling (Ciamporova & Mistrik, 1993; Glinska *et al*., 2009), salinity (Wojtyla *et al*., 2013), heat (Pareek *et al*., 1997), water deficit (Mistrik *et al*., 1992). The effects are usually expressed by the formation of rings or whorls in the ER membrane or dilation of ER cisternae. In the present study, the exposure of meristematic cells of both plants to low pH initially resulted in aggregations of ER membranes along the cell periphery and finally in dilation of ER cisternae, accompanied by the presence of electron-dense material among them. These phenomena could be connected to the synthesis of proteins under various stressed conditions (Pareek *et al*., 1997). The electron-dense material could result from increased synthesis of phenolic compounds (Stefanowska *et al*., 2003), as their necessary enzymes are present on ER membranes (Wagner & Hrazdina, 1984). This is further supported by the fact that high levels of CO_2 trigger accumulations of plant phenolic protective substances (Arnold *et al*., 2012). Alternately, it has been proposed that there is a connection between reorganization of ER and the level of respiratory products (probably ATP) when is limited or lacking (Kolb *et al*., 2004), suggesting that in OA stress this reorganization may result from limited metabolic activity.

The high number of dictyosomes in *C. nodosa* cells, even after only one week, as well as their enlarged and extended vesicles, was also observed under salt stress of lupine embryos (Wojtyla *et al*., 2013), cold-stressed soybeans (Glikska *et al*., 2009) as well as after treatment with H_2O_2 (Darehshouri *et al*., 2008). It has been suggested that their appearance might be related to disturbances of secretion process (Glikska *et al*., 2009) or to PCD (Darehshouri *et al*., 2008).

The question arises is whether these responses are governed by controlled cellular processes, particularly PCD. It should be noted that PCD is a physiological cell death event leading to the selective elimination of cells which are unwanted, unnecessary, or have exhausted their functions (Ellis *et al*., 1991; Pennell & Lamb, 1997). However, there are types of PCD operating in plants that are not as clearly defined and thus are not assigned to a specific type of PCD.

Moreover, in the present study, the MT network was investigated, as MTs are proposed as "elements of a sensory hub that decodes stress-related signal signatures" (Nick, 2013). In this study, long-term incubation at low pH was shown to influence MTs in interphase cells. It is proposed that cytoskeletal changes are related to signalling events in response to stress factors (Muller *et al*., 2007; Koutalianou *et al*., 2016).

The alterations to organelle structure caused by low pH described in the present study (i.e., fragmented DNA and chromatin condensation, enlargement of ER and increased number of swollen mitochondria) are similar to those observed in normal PCD processes such as tapetal development (Papini *et al*., 1999) or another type of tissue premature cell death (Balk & Leaver, 2001), with a

notable difference in mitochondria which in the tapetal and another cells persist until quite late.

Conclusion

We can conclude that the cell and organelle degradation and MT disturbance occurring in the seagrasses *C. nodosa* and *P. oceanica* after a short-term (3 weeks) low pH treatment (acidification) could be considered comparable to an apoptotic-like PCD phenomenon. However, it is still unclear whether the function of PCD is to protect the plant's life by sacrificing some part of cells, or whether it is mainly due to damage accumulation during severe stress. Whatever the case, this study does clearly demonstrate that both *P. oceanica* and *C. nodosa* seem to be relatively poorly adapted to a rapid pH change. Further experiments, including recovery experiments after long-term stress, need to be conducted to investigate the tolerance of these two species and to obtain data on apoptotic-like PCD phenomena in the survival of these two pioneering species.

Acknowledgements

The authors wish to express their thanks to Prof. Konstantinos Fasseas (Agricultural University of Athens) for the access to TEM facilities. The authors also wish to thank Giovanna Benvenuto for access to confocal microscopy facilities (Stazione Zoologica Anton Dohrn, Napoli, Italy). This work was supported by the European Union (European Social Fund – ESF), National funds through the Operational Program "Education and Lifelong Learning" of the National Strategic Reference Framework (NSRF) - Research Funding Program: THALES (MIS: 375425), the University of Athens (program "Kapodistrias") and the ASSEMBLE – Association of European Marine Biological Laboratories- grant agreement no. 227799 at Stazione Zoologica Anton Dohrn (Napoli). This work is part of the research program LTER-LA, supported by the Stazione Zoologica Anton Dohrn.

Conflict of interest. The authors declare that they have no conflict of interest.

References

Adamakis, D.I., Malea, P., Panteris, E., 2018. The effects of Bisphenol A on the seagrass *Cymodocea nodosa*: Leaf elongation impairment and cytoskeleton disturbance. *Ecotoxicology and Environmental Safety,* 15 (157), 431-440.

Adamakis, D.I., Malea, P., Sperdouli, I., Panteris, E., Kokkinidi, D. *et al.,* 2021. Evaluation of the spatiotemporal effects of bisphenol A on the leaves of the seagrass *Cymodocea nodosa*. *Journal of Hazardous Materials*, 404, 124001.

Apostolaki, E.T., Vizzini, S., Hendriks, I., Olsen, Y.S., 2014. Seagrass ecosystem response to long-term high CO_2 in a Mediterranean volcanic vent. *Marine Environmental Research*, 99, 9-15.

Arnold, T., Mealey, C., Leahey, H., Miller, W., Hall-Spencer, J.M. *et al.,* 2012. Ocean acidification and the loss of phenolic substances in marine plants. *PLoS One,* 7, 1-10.

Austin, J.R., Frost, E., Vidi, P.A., Kessler, F., Staehelin, L.A., 2006. Plastoglobules are lipoprotein subcompartments of the chloroplast that are permanently coupled to thylakoid membranes and contain biosynthetic enzymes. *The Plant Cell,* 18 (7), 1693-1703.

Balk, J., Leaver, C.J., 2001. The PET1-CMS mitochondrial mutation in sunflower is associated with premature programmed cell death and cytochrome c release. *The Plant Cell,* 13, 1803-1818.

Barber, B.J., Behrens, P.J., 1985. Effects of elevated temperature on seasonal *in situ* leaf productivity of *Thalassia testudinum* Banks ex Konig and *Syringodium filiforme* Kutzing. *Aquatic Botany,* 22, 61-69.

Barnabas, A.D., Butler, V., Steinke, T.D., 1977. *Zostera capensis* Setchell. I. Observations of the fine structure of the leaf epidermis. *Zeitschrift für Pflanzenphysiologie,*85, 417-427.

Beal, J.L., Schmit, B.S, 2000. The effects of dock height on light irradiance (PAR) and seagrass (*Halodule wrightii* and *Syringodium filiforme*) cover, *In*: (Bortone, S.A. ed.), Seagrasses: monitoring, ecology, physiology, and management. Boca Raton, Florida CRC *Marine Science Series,* 49-63.

Beer, S., Koch, E., 1996. Photosynthesis of marine macroalgae and seagrasses in globally changing CO_2 environments. *Marine Ecology Progress Series,* 141, 199-204.

Benjamina, K.J., Walkerb, D., McComb, A., Kuo., J., 1999. Structural response of marine and estuarine plants of *Halophila ovalis* (R. Br.) Hook. f. to long-term hyposalinity. *Aquatic. Botany,* 64, 1-17.

Bennici, A., Tani, C., 2012. Ultrastructural characteristics of callus cells of *Nicotiana tabacum* L. var. BELW3 grown in presence of NaCl. *Caryologia,* 65, 72-81.

Buia, M.C., Zupo, V., Mazzella, L., 1992. Primary production and growth dynamics in *Posidonia oceanica*. *Marine Ecology,* 13, 2-16.

Cancemi, G., Buia, M.C., Mazzella, L., 2002. Structure and growth dynamics of *Cymodocea nodosa* meadows. *Scientia Marina,* 66, 365-373.

Carpenter, K.E., Muhammad, A., Greta, A., Aronson, R., Banks, S. *et. al.,* 2008. One-Third of Reef-Building Corals Face Elevated Extinction Risk from Climate Change and Local Impacts. *Science*, 321(5888), 560-563.

Ciamporova, M., Mistrik, I., 1993. The ultrastructural response of root cells to stressful conditions. *Environmental and Experimental Botany,* 33, 11-26.

Cornwall, C.E., Hepburn, C.D., McGraw, C.M., Currie, K.I., Pilditch, C.A. *et al.,* 2013. Diurnal fluctuations in seawater pH influence the response of a calcifying macroalga to ocean acidification. *Proceedings of the Royal Society B: Biological Sciences,* 280, 20132201.

Darehshouri, A., Affenzeller, M., Lütz-Meindl., U., 2008. Cell death in the unicellular green alga *Micrasterias* upon H_2O_2 induction. *Plant Biology*, 10 (6), 732-745.

Daud, M.K., Variath, M.T., Ali, S., Najeeb, U., Jamil, M. *et. al.,* 2009. Cadmium-induced ultramorphological and physiological changes in leaves of two transgenic cotton cultivars and their wild relative. *Journal of Hazardous Material,*

168 (2-3), 614-625.

Doohan, M., Newcomb, H., 1976. Leaf ultrastructure and δ13C values of three seagrasses from the Great Barrier Reef. *Australian Journal of Plant Physiology,* 3, 9-23.

Easterling, D.R., Meehl, G.A., Parmesan, C., Changnon, S.A., Karl, T.R. *et al.,* 2000. Climate extremes: observations, modeling, and impacts. *Science,* 289, 2068-2074.

Ellis, R.E., Yuan, J., Horvitz. H.R., 1991. Mechanisms and functions of cell death. *Annual Review of Cell and Developmental Biology*, 7, 663-698.

Foo, S.A., Byrne, M., Ricevuto, E., Gambit, M.C., 2018. The carbon dioxide vents of Ischia, Italy, a natural system to assess impacts of ocean acidification on marine ecosystems: an overview of research and comparison with other vent systems. *Oceanography and Marine Biology*: An Annual review, 56, 237-310.

Eymery, F., Rey, P., 1999. Immunocytolocalization of CDSP 32 and CDSP 34, two chloroplastic drought-induced stress proteins in *Solanum tuberosum* plants. *Plant Physiology and Biochemistry,* 37, 305-312.

Fabricius, K.E., Langdon, C., Uthicke, S., Humphrey, C., Noonan, S. *et al.,* 2011. Losers and winners in coral reefs acclimatized to elevated carbon dioxide concentrations. *Nature Climate Change,* 1, 165-169.

Garrard, S.L., Gambi, M.C., Scipione, M.B., Patti, F.P., Lorenti, M. *et al.,* 2014. Indirect effects may buffer negative responses of seagrass invertebrate communities to ocean acidification. *Journal of Experimental Marine Biology and Ecology,* 461, 31-38.

Gattuso, J.P., Mach, K.J., Morgan. G., 2013. Ocean acidification and its impacts: an expert survey. *Climate Change,* 117, 725-738.

Glinska, S., Gapinska, M., Gabara, B., Mikicinski, A., Szafranska, K., 2009. Effects of chilling on the root cell ultrastructure of two soybean cultivars. *Journal of Plant Biology,* 53, 539-544.

Grigorova, B., Vassileva, V., Klimchuk, D., Vaseva, I., Demirevska, K., 2012. Drought high temperature and their combination affect ultrastructure of chloroplasts and mitochondria in wheat (*Triticum aestivum* L.) leaves. *Journal of Plant Interactions,* 7, 204-213.

Hall-Spencer, J.M., Rodolfo-Metalpa, R., Martin, S., Ransome, E., Fine, M. *et al.,* 2008. Volcanic carbon dioxide vents show ecosystem effects of ocean acidification. *Nature,* 454, 96-99.

Harley, C.D., Anderson, G.M., Demes, K.W., Jorve, J.P., Kordas, R.L., 2012. Effects of climate change on global seaweed communities. *Journal of Phycology,* 48, 1064-1078.

Hendriks, I.E., Olsen, Y.S., Duarte, C., 2017. Light availability and temperature, not increased CO_2, will structure future meadows of *Posidonia oceanica*. *Aquatic Botany*, 139, 32-36.

IPCC, 2013. Emissions scenarios. A special report of Working Group III of the Intergovernmental Panel on Climate Change. *Cambridge University Press*, Cambridge, p 599.

IPCC, 2021. Climate Change 2021. The Physical Science Basis. Contribution of Working Group I to the Sixth Assessment Report of the Intergovernmental Panel on Climate Change [Masson-Delmotte, V., P. Zhai, A. Pirani, S. L. Connors, C. Péan, S., Berger, N., Caud, Y., Chen, L., Goldfarb, M.I., Gomis, M., Huang, K., Leitzell, E., Lonnoy, J.B.R., Matthews, T.K., Maycock, T., Waterfield, O., Yelekçi, R.Yu and B. Zhou (Eds.)]. Cambridge University Press. In Press.

Iyer, V., Barnabas, A.D., 1993. Effects of varying salinity on leaves of *Zostera capensis* Setchell. I. Ultrastructural changes. *Aquatic Botany,* 46 (2), 141-153.

Jagels, R., Barnabas, A.D., 1989. Variation in leaf ultrastructure of *Ruppia maritima* L. along a salinity gradient. *Aquatic Botany*, 33, 207-221.

Jiang, Z.J., Huang, X.P., Zhang, J.P., 2010. Effects of CO_2 enrichment on photosynthesis, growth, and biochemical composition of seagrass *Thalassia hemprichii* (Ehrenb.) Aschers. *Journal of Integrative Plant Biology,* 52, 904-913.

Johnson, V.R., Russell, B.D., Fabricius, K.E., Brownlee, C., Hall-Spencer, J.M., 2012. Temperate and tropical brown macroalgae thrive, despite decalcification, along natural CO_2 gradients. *Global Change Biology,* 18, 2792-2803.

Kanwischer, M., Porfirova, S., Bergmuller, E., Dormann, P., 2005. Alterations in tocopherol cyclase activity in transgenic and mutant plants of *Arabidopsis* affect tocopherol content, tocopherol composition and oxidative stress. *Plant Physiology,* 137, 713-723.

Katsaros, C., Galatis, B., Mitrakos, K., 1983. Fine structural studies on the interphase and dividing apical cells of *Sphacelaria tribuloides* (Phaeophyta). *Journal of Phycology*, 19,16-30.

Katsaros, C., Galatis, B., 1992. Immunofluorescence and electron microscopic studies of microtubule organization during the cell cycle of *Dictyota dichotoma* (Phaeophyta, Dictyotales). *Protoplasma* 169, 75-84.

Kerrison, P., Hall-Spencer, J.M., Suggett, D.J., Hepburn, L.J., Steinke, M., 2011. Assessment of pH variability at a coastal CO_2 vent for ocean acidification studies. *Estuarine, Coastal and Shelf Science*, 94, 129-137.

Keser, M., Swenarton, J.T., Foertch. J.F., 2005. Effects of thermal input and climate change on growth of *Ascophyllum nodosum* (Fucales, Phaeophyceae) in eastern Long Island Sound (USA). *Journal of Sea Research,* 54, 211-220.

Koch, M., Schopmeyer, S., Kyhn-Hansen, C., Madden. C.J., 2007. Synergistic effects of high temperature and sulfide on tropical seagrass. *Journal of Experimental Marine Biology and Ecology,* 341, 91-101.

Koch, M., Bowes, G., Ross, C., Zhang, X.H., 2013. Climate change and ocean acidification effects on seagrasses and marine macroalgae. *Global Change Biology,* 19 (1), 103-32.

Kolb, R.M., Dolder, H., Cortelazzo, A.L., 2004. Effects of anoxia on root ultrastructure of four neotropical trees. *Protoplasma,* 224, 99-105.

Koutalianou, M., Orfanidis, S., Katsaros, C., 2016. Effects of high temperature on the ultrastructure and microtubule organization of interphase and dividing cells of the seagrass *Cymodocea nodosa*. *Protoplasma,* 253 (2), 299-310.

Kroeker, K.J., Kordas, R.L., Crim, R.N., Singh, G.G., 2010. Meta-analysis reveals negative yet variable effects of ocean acidification on marine organisms. *Ecology Letters,* 13, 1419-1434.

Kroeker, K.J., Micheli, F., Gambi, M.C., Martz, T.R., 2011. Divergent ecosystem responses within a benthic marine community to ocean acidification. *Proceedings of the National*

Academy of Sciences of USA, 108, 14515-14520.

Kumar, A., Buia, M.C., Palumbo, A., Mohany, M., Wadaan, M.A.A., *et al.,* 2020. Ocean acidification affects biological activities of seaweed: A case study of *Sargassum vulgare* from Ischia volcanic CO_2 vents. *Environmental Pollution*, 259, 138896.

Kuo, J., 1978. Morphology, anatomy and histochemistry of the Australian seagrasses of the genus *Posidonia* Konig (Posidoniaceae) I. Leaf blade and leaf sheath of *Posidonia australis* Hook f. *Aquatic Botany,* 5, 171-190.

Kuo, J., Ridge, R., Lewis, S., 1990. The leaf internal morphology and ultrastructure of *Zostera muelleri* Irmisch ex Aschers. (Zosteraceae): a comparative study of the intertidal and subtidal forms. *Aquatic Botany,* 36, 217-236.

Kuo, J., 1993. Functional leaf anatomy and ultrastructure in a marine angiosperm, *Syringodium isoetifolium* (Aschers.) Dandy (Cymodoceaceae). *Australian Journal of Marine and Freshwater Research*, 44, 59-73.

Kuo, J., Den Hartog, C., 2006. Seagrass morphology, anatomy, and ultrastructure. *In*: (Larkum, AWD. ed.) Seagrasses: biology, ecology and conservation. Springer, Netherlands pp. 51-87.

Kvitt, H., Kramarsky-Winter, E., Maor-Landaw, K., 2015. Breakdown of coral colonial form under reduced pH conditions is initiated in polyps and mediated through apoptosis *Proceedings of the National Academy of Sciences of. USA,* 112, 2082-2086.

Larkum, W.D., Orth, R.J., Duarte, C.M., 2006. Seagrasses: Biology, Ecology and Conservation. Dordrecht (The Netherlands), Springer.

Lee, K.S., Dunton, K.H., 1997. Effects of *in situ* light reduction on the maintenance, growth and partitioning of carbon resources in *Thalassia testudinum* Banks ex Konig. *Journal of Experimental Marine Biology and Ecology,* 210, 53-73.

Lee, S.H., Singh, A.P., Chung, G.C., Kim, Y.S., Kong, I.B., 2002. Chilling root temperature causes rapid ultra-structural changes in cortical cells of cucumber (*Cucumis sativus* L.) root tips. *Journal of Experimental Botany,* 53, 2225-2237.

Le Rudulier, D., Strøm, A.R., Dandekar, A.M., Smith, L.T., Valentine, R.C., 1984. Molecular biology of osmoregulation. *Science,* 244, 1064-1068.

Li, Z., Xing, D., 2011. Mechanistic study of mitochondria-dependent programmed cell death induced by aluminium phytotoxicity using fluorescence techniques. *Journal of Experimental Botany,* 62, 331-34.

Mackey, B., DellaSala, D.A., Kormos, C., Lindenmayer, D., Kumpel, N. *et al.,* 2015. Policy options for the world's primary forests in multilateral environmental agreements. *Conservation Letters*, 8 (2), 139-147.

Malea, P., Adamakis, S., Kevrekidis, T., 2013. Microtubule integrity and cell viability under metal (Cu, Ni and Cr) stress in the seagrass *Cymodocea nodosa*. *Chemosphere* 463, 611-623.

Mannela, C.A., 2008. Structural diversity of mitochondria: functional implications. *Annals of the New York Academy of Sciences,* 1147, 171-179.

Mascaró, O., Oliva, S., Pérez, M., Romero, J., 2009. Spatial variability in ecological attributes of the seagrass *Cymodocea nodosa*. *Botanica Marina,* 52, 429-438.

Mazzella, L., Scipione, M.B., Buia, M.C., 1989. Spatio Temporal Distribution of Algal and Animal Communities in a *Posidonia oceanica* Meadow. *Marine Ecology*, 10 (2), 107-129.

Mistrik, M., Holobrada, M., Čiamporova. M., 1992. The root in unfavourable conditions. In Physiology of the plant root system, (J. Kolek, V. Kozinka Eds.), *Kluwer Academic, Dordrecht*, 286-312.

Mora, C., Wei, C.L., Rollo, A., Amaro, T., Baco, A.R. *et al.,* 2013. Biotic and Human Vulnerability to Projected Changes in Ocean Biogeochemistry over the 21st Century. *Plos Biology,* 11 (10), e1001682.

Muller, J., Menzel, D., Samaj, J., 2007. Cell type specific disruption and recovery of cytoskeleton in *Arabidopsis thaliana* epidermal root cells upon heat shock stress. *Protoplasma*, 230-242.

Mylona, Z., Panteris, E., Moustakas, M., Kevrekidis, T., Malea, P., 2020a. Physiological, structural and ultrastructural impacts of silver nanoparticles on the seagrass *Cymodocea nodosa*. *Chemosphere,* 248, 126066.

Mylona, Z., Panteris, E., Kevrekidis, T., Malea, P., 2020b. Physiological and structural responses of the seagrass *Cymodocea nodosa* to titanium dioxide nanoparticle exposure. *Botanica Marina*, 6, 493-507.

Nick, P., 2013. Microtubules, signaling and abiotic stress. *The Plant Journal,* 75,309-323.

Ondiviela, B., Losada, I., Lara, J., Mazaa, M., Galvána, C., *et al.,* 2014. The role of seagrasses in coastal protection in a changing climate. *Coastal Engineering,* 87, 158-168.

Orr, J.C., Fabry, V.J., Aumont, O., Bopp, L., Doney, S.C. *et al.,* 2005. Anthropogenic ocean acidification over the twenty-first century and its impact on calcifying organisms. *Nature,* 437, 681-686.

Orth, R.J., Carruthers, T.J., Dennison, W.C., Duarte, C.M., Fourqurean, J.W. *et al.,* 2006. A global crisis for seagrass ecosystems. *Bioscience,* 56, 987-996.

Panda, S.K., Yamamoto, Y., Kondo, H., Matsumoto, H., 2008. Mitochondrial alterations related to programmed cell death in tobacco cells under aluminium stress. *Comptes Rendus Biologies,* 331 (8), 597-610.

Papini, A., Mosti, S., Brighigna, K., 1999. Programmed cell death events during tapetum development of angiosperms. *Protoplasma*, 207, 213-221.

Pennell, R.I., Lamb, C., 1997. Programmed cell death in plants. *The Plant Cell,* 9, 1157-1168.

Pareek, A., Singla, S., Grover, A., 1997. Short-term salinity and high temperature stress-associated ultrastructural alterations in young leaf cells of *Oryza sativa* L. *Annual Botany,* 80, 629-639.

Pergent, G., Bazairi, H., Bianchi, C.N., Boudouresque, C.F., Buia, M.C. *et al.,* 2014. Climate change and Mediterranean seagrass meadows: a synopsis for environmental managers. *Mediterranean Marine Science,* 15 (2), 462-473.

Porzio, L., Buia, M.C., Hall-Spencer, J.M., 2011. Effects of ocean acidification on macroalgal communities. *Journal of Experimental Marine Biology and Ecology,* 400, 278-287.

Porzio, L., Garrard, SL., Buia, MC., 2013. The effect of ocean acidification on early algal colonization stages at natural CO_2 vents. *Marine Biology,* 160, 2247-2259.

Procaccini, G., Beer, S., Bjork, M., Olsen, J., Mazzuca, S., *et al.,*2012. Seagrass ecophysiology meets ecological genomics: are we ready? *Marine Ecology,* 33, 522-527.

Ralph, P.J., 1998. Photosynthetic responses of *Halophila ovalis* (R Br.) Hook. F. to osmotic stress. *Journal of Experimental Marine Biology and Ecology*, 227(2),203–220.

Ravaglioli, C., Lauritano, C., Buia, M.C., Balestri, E., Capocchi, A. *et al.,* 2017. Nutrient enrichment offsets negative effects of ocean acidification in seagrass meadows. *Scientific Reports,* 7, 13732.

Reape, T.J., McCabe, P.F., 2008. Apoptotic-like programmed cell death in plants. *New Phytologist,* 180, 13-26.

Reusch, T.B.H., 2013. Climate change in the oceans: evolutionary versus phenotypically plastic responses of marine animals and plants. *Evolutionary Applications,* 7 (1), 104-122.

Riebesell, U., 2008. Acid test for marine biodiversity. *Nature,* 454, 46-47.

Ries, J.B., Cohen, A.L., McCorkle, D.C., 2009. Marine calcifiers exhibit mixed responses to CO_2-induced ocean acidification. *Geology*, 37,1131-1134.

Rurek, M., 2014. Plant mitochondria under a variety of temperature stress conditions. *Mitochondrion,* 19, 289-294.

Scartazza, A., Moscatello, S., Gavrichkova, O., Buia, M.C., Lauteri, M. *et al.,* 2017. Carbon and nitrogen allocation strategy in *Posidonia oceanica* is altered by acidification. *Science of The Total Environment*, 607, 954-964.

Serra, I.A., Nicastro, S., Mazzuca, S., Natali, L., Cavallini, A. *et al.,* 2013. Response to salt stress in seagrasses: PIP1;1 aquaporin antibody localization in *Posidonia oceanica* leaves. *Aquatic Botany,* 104, 213-219.

Stefanowska, M., Kuras, M., Kacperska, A., 2002. Low temperature induced modifications in cell ultrastructure and localization of phenolics in water oilseed rape (*Brassica napus* L. var. oleifera L.) leaves. *Annals of Botany,* 90, 637-645.

Tedesco, D., 1996. Chemical and isotopic investigations of fumarolic gases from Ischia Island (southern Italy): evidence of magmatic and crustal contribution. *Journal of Volcanology and Geothermal Research,* 74, 233-242.

Tsioli, T., Papathanasiou, V., Rizouli, A., Kosmidou, M., Katsaros, C. *et al.,* 2021. Diversity and composition of algal epiphytes on the Mediterranean seagrass *Cymodocea nodosa*: a scale-based study. *Botanica Marina,* 2, 64-70.

Uthicke, S., Momigliano, P., Fabricius, K., 2013. High risk of extinction of benthic foraminifera in this century due to ocean acidification. *Scientific Reports,* 3, 1769, 1-5.

Vizzini, S., Tomasello, A., Di Maida, G., Pirrotta, M., Mazzola, A., 2010. Effect of explosive shallow hydrothermal vents on $d^{13}C$ and growth performance in the seagrass *Posidonia oceanica*. *Journal of Ecology,* 98, 1284-1291.

Wagner, G.J., Hrazdina. G., 1984. Endoplasmic reticulum as a site of phenylpropanoid and flavonoid metabolism in *Hippeastrum*. *American Society of Plant Biologists,* 74 (4), 901-906.

Waycott, M., Duarte, CM., Carruthers, T.J.B., Orth, R.J., Dennison, W.C., *et al.,* 2009. Accelerating loss of seagrasses across the globe threatens coastal ecosystems. *Proceedings of the National Academy of Sciences of the USA,* 106, 12377-12381.

Wei, L., Wang, Q., Ning, X., Mu, C., Wang, C. *et al.,* 2015. Combined metabolome and proteome analysis of the mantle tissue from Pacific oyster *Crassostrea* gigas exposed to elevated pCO_2. *Comparative Biochemistry and Physiology Part D: Genomics & Proteomics*, 13, 16-23.

Wojtyla, L., Rucinska-Sobkowiak, R., Kubala, S., Garnczarska. M., 2013. Lupine embryo axes under salinity stress. I. Ultrastructural response. *Acta Physiologiae Plantarum,* 35, 2219-2228.

Wu, J.-X., Cheng, X., Xiao, H.-S, Wang, H., Yang, L.-Z. *et al.,* 2008. Agricultural landscape change in China's Yangtze Delta, 1942-2002: A case study. *Agriculture, Ecosystems & Environment*, 129, 523-533.

York, P., Gruber, R., Hill, R., Ralph, P., Booth, D. *et al.,* 2013. Physiological and morphological responses of the temperate seagrass *Zostera muelleri* to multiple stressors: investigating the interactive effects of light and temperature. *PLoS One,* 8(10), e76377.

Zupo, V., Buia, MC., Mazzella, L., 1997. A production model for *Posidonia oceanica* based on temperature. *Estuarine, coastal and shell science*, 44, 483-492.

Supplementary Data

The following supplementary information is available online for the article:

Suppl. Fig. 1: Variability of seawater pH on the southern side of the Castello Aragonese (from Porzio *et al.,* 2011).
Suppl. Fig. 2: Plastic frame with iron bar used for the experimental procedure at area S1 (A), area S2 (B) and area S3 (C).
Suppl. Fig. 3: Water temperature in June and July (experimental period), matching ambient seasonal fluctuations (13-25°C).
Suppl. Fig. 4: Weekly mean values of pH recorded at the three vents sites, varying from 8.08 ±0.004 (S1) to 7.71 ±0.133 (S2) to 6.584 ±0.145 (S3).
Suppl. Fig. 5: Histogram showing the number of mitochondria in epidermal cells in *C. nodosa* in the control area and in S2 and S3 areas. Transfer for one week in S2 resulted in a slight increase of the number of mitochondria per cell; at S3 mitochondria were three times as abundant compared to the control.
Suppl. Fig. 6: Histogram showing the number of dictyosomes in epidermal cells in *C. nodosa* in the control area and after one week in S1 and S2 areas.
Suppl. Fig. 7: Histogram showing the percentage of dictyosomes with a specific number of cisternae (2-4 and 5-9) in epidermal cells in *C. nodosa* in the control area and after one week in S2 and S3 areas. After one week in S2 and S3 areas the number of dictyosomes with 5-9 cisternae was increased to four times that of the control.